Reversible Enhancement of Reversibly Data Embedded Images using HVS Characteristics of DCT

Rebecca Dhupppe *rebeccadhuppe@gmail.com*
Assistant Professor
Department of CSE
Vardhaman College of Engineering,
Hyderabad, 501218, India

Dr. Sagar Gujjunoori *sagar4u.nitk@gmail.com*
Professor
Department of CSE
Vardhaman College of Engineering,
Hyderabad, 501218, India

Gouthaman KV *gouthamankv@gmail.com*
Junior Research Fellow
Department of CSE
Vardhaman College of Engineering,
Hyderabad, 501218, India

Bharathi Ghosh *bharathighosh2511@gmail.com*
Assistant Professor
Department of CSE
Vardhaman College of Engineering,
Hyderabad, 501218, India

Abstract

In the recent, HVS based reversible data embedding is emerging. In a reversible data embedding scheme, in the process of achieving reversibility and embedding the data, it induces some distortions into marked image/video. If the distortions in marked image are random due to reversible embedding, it may not reveal much information about the existence of hidden data; on the contrary, if the distortions are repetitive geometric patterns which arises when an embedding scheme's emphasis is on capacity and reversibility, then the marked media with geometric distortions may reveal the existence of the hidden data. Further, in applications involving satellite images, medical, military, fine arts images, etc. which involves reversible embedding, it requires to show the details for inspection. Due to repetitive geometric distortions as in [6] and [7], the visual quality of image degrades. Hence, there is a need for enhancing the reversibly embedded images. To tackle this issue, if any exiting image enhancement scheme is used, it incur in loss of hidden data as well as the restoration of image to original form is not possible; hence, violating the requirement of reversibility for such applications. To address this problem we propose a reversible image enhancement scheme for reversibly data embedded images by using HVS characteristics of DCT. The experimental results show that the visual quality has been improved in terms of PSNR, PSNR-HVS, PSNR-HVS-M, and MSSIM when compared to S. Gujjunoori et al. scheme [6] and S. Gujjunoori et al. scheme [7], which contains repetitive geometrical distortions in marked media.

Keywords: Reversible Enhancement, DCT, HVS Characteristics, Visual Quality, Reversible Data Embedding.

1. INTRODUCTION

Advances in computing, communication and storage technologies made apparent that a layman could be able to opt for technology enabled devices, resulting in wide usage of digital devices. In particular, the use of multimedia data such as image, video, audio, etc. has been intensified due to the evolution in digital storage and communication. In the recent, we substantiate an evolutionary growth of YouTube, E-learning and Web conferencing sites and many more. The use of multimedia data in social media such as facebook, twitter, flickr, skype, whatsapp, etc. has been extensively intensified in this decade. A greater number of applications directly or indirectly associated with processing of images, video, audio, etc. which in turn generating new security challenges in terms of privacy, authentication, etc. Data embedding (watermarking or steganography) has become a tool for addressing the security challenges in multimedia storage and communication [4], [6].

There exists many data embedding schemes, broadly classified into irreversible [1, 2, 5, 14] and reversible [3, 9, 11, 12, 15-19]. The major requirement of data embedding schemes is to achieve higher capacity, visual quality and robustness [4]. But there exists a triangular trade-off between these parameters. Many schemes in the literature focus on one requirement by compromising the other requirement.

Especially, when capacity and visual quality is concern, increasing capacity reduces visual quality and vice versa. If the visual quality is also improved while embedding the data, it is well and good. If the care is not taken towards improving the visual quality while the focus is on increasing the capacity or other parameters, then there is a need to explicitly enhancing the visual quality. Since, the distortions induced in marked image or video while achieving high capacity may reveal the existence of hidden data. Further, in applications involving satellite images, medical, military, fine arts images, etc. which involves reversible embedding, it requires to show the details for inspection [18]. Due to repetitive geometric distortions as in [6] and [7], the visual quality of image degrades and the distortions may reveal the existence of hidden data. Hence there is need for enhancing the embedded images/videos. Enhancement can be irreversible or reversible. If the enhancement is irreversible, where the existing enhancement techniques can be explicitly applied, then it incur in loss of hidden data. If the enhancement is reversible, then there will not be any loss to the hidden data in marked image or video. Enhancement can be performed for images/videos which contain hidden data embedded in spatial domain or frequency domain. Our focus is on enhancing the images which contain hidden data in quantized DCT coefficients by a reversible data embedding scheme. Discrete Cosine Transformation (DCT) based data embedding has become very popular for the reason that the DCT is widely used in compression standards such as JPEG, MPEG, JVT, H.261, etc. and embedding the data into frequency domain enables to achieve robustness [6-8, 10, 13].

Recently, HVS based reversible data embedding schemes are emerging. The HVS based reversible data embedding schemes focus on achieving better visual quality of the marked image or video by utilizing the underlying HVS characteristics of DCT, while maintaining the reversibility and increasing the hiding capacity as in S. Gujjunoori et al. schemes [6, 7]. The reversible data embedding schemes by S. Gujjunoori et al. [6, 7] are aimed to limit the trade-off exists between embedding capacity and visual quality maintaining reversibility, by embedding the data in middle frequency quantized DCT coefficients. In S. Gujjunoori et al. [6], the data is embedded by choosing a random sign, + or -, when secret bit is 1. This resulted in additional modifications to the non-zero AC coefficients while eliminating the ambiguity. Later, S. Gujjunoori et al. [7] have proposed a reversible scheme by avoiding the alteration of non-zero negative AC coefficients to improve the visual quality. However, both the schemes [6] and [7] by S. Gujjunoori et al., focus on HVS based reversible embedding in DCT domain, introduce geometrical distortions in smoother regions of the marked video/image, as shown in Figure 1. These geometrical distortions in the marked image may reveal the existence of hidden data, which violates the vary purpose of invisible data hiding.

FIGURE 1: Geometrical distortions by S. Gujjunoori et.al scheme [6].

Hence, there is a need for enhancing the embedded images whenever the care is not taken while the focus is on other parameters such as HVS characteristics of DCT and improving the capacity as in [6]. The reversible image enhancement schemes must be designed by considering a specific data embedding scheme; one cannot apply any other enhancement scheme in this scenario. In this paper, we propose a reversible enhancement scheme for reversibly data embedded images using HVS characteristics of DCT. To best of our knowledge, there is no existing reversible image enhancement scheme with respect to an embedding scheme.

2. THE PROPOSED SCHEME

The proposed scheme enhances the visual quality of reversibly embedded image by S. Gujjunoori et al. schemes [6, 7]. In the proposed scheme, both spatial domain and frequency domain are considered; image enhancement is carried out in spatial domains and DC coefficients of the frequency domain are used for choosing the regions of embedded image for enhancement with respect to different shades of gray scale image such as, dark, gray and bright. To convert an image from spatial domain to frequency domain, the 2D DCT [13] as in equation (1) is applied on an image lock after level offsetting by a value 128.

$$G_{u,v} = \frac{\propto (u) \propto (v)}{4} \sum_{x=0}^{7} \sum_{y=0}^{7} I(x,y) g(x,y,u,v) \tag{1}$$

where

$$g(x,y,u,v) = cos\left(\frac{(2x+1)u\pi}{16}\right) cos\left(\frac{(2y+1)v\pi}{16}\right)$$

$$\propto (z) = \begin{cases} \frac{1}{\sqrt{2}} & if\ z = 0, \\ 1 & if\ z \neq 0. \end{cases}$$

In equation (1), I be a block of the image in spatial domain and $G_{u,v}$ be the DCT coefficient at coordinates (u,v) in frequency domain. Here, $0 \leq u,v \leq 7$. Let the size of the image be$M \times N$, then there are $l = \frac{M \times N}{64}$ number of 8×8 blocks. Assuming the size of the image is of multiple of eight. Let D_i be the DC coefficient value from the frequency domain representation of$I$, where, $0 \leq i \leq l$.

We observed in [6] and [7] that the repetitive geometric distortions more apparent in bright and dark smoother regions of an embedded image than in gray and textured regions. So, instead of enhancing the geometrical distortions every block, image enhancement mechanism is carried out only on smoother dark and bright regions. We use the DC values of a quantized DCT block, whose values is between -128 to 127 after level offsetting the pixel by 128; called a DC threshold range. Where, the DC threshold range is referred as the range of DC coefficients of dark regions to bright regions of an embedded image.

The threshold values for choosing the smoother bright and dark regions are considered by observing the DC coefficient histogram as in Figure 2b, 3b and 4b. Let T_d and T_b are the threshold values for dark and bright regions respectively. All the DC coefficients less than or equal to T_d are considered as of dark regions. Also, all the DC coefficients greater than or equal to T_b are considered as of bright regions.

The T_d and T_b value of the images varies according to the different images, since the DC coefficient histogram changes based on the local content of the images as shown in Figures 2b, 3b and 4b. The T_d and T_b value of the Parrots image is -32 and 25 respectively, shown in Table 1. From the Figure 5b it is observed that the DC coefficient -46 is less than T_d = -32 hence, it has smoother dark regions as shown in Figure 5a. Similarly, from the Figure 6b it is observed that the DC coefficient 36 is greater than T_d = 25 hence, it is a bright region which is shown in Figure 6a.

TABLE 1: DC Threshold Range.

Test Images	Threshold range(T_d: T_b)
Bird	-35:15
Arts	-30:20
Parrots	-32:25
Multi	-55:25
Fish	-60:15
Man	-50:25
Mansion	-40:20
Cycle	-30:20
Perm	-50:25
Stars	-40:20
Sydney	-30:20
Univ	-30:20

The proposed scheme is shown in Figure 7. From Figure 7, we can observe that the reversible enhancement scheme lies between data embedding and data extraction schemes, which imply that the image enhancement is performed after embedding the data at sender side using a specific data embedding scheme. Similarly, the reversible operation, restoration is performed before extracting the data at receiver end. Here, we use S. Gujjunoori et al. data embedding schemes [6, 7]. The enhancement and restoration procedures are detailed in sections 2.1 and 2.2 respectively.

(a) (b)

FIGURE 2: (a) Test Image (Man) (b) DC coefficient histogram of test Image (Man).

(a)

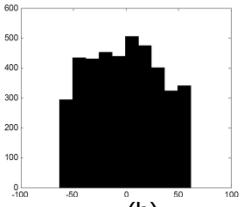

(b)

FIGURE 3: (a) Test Image (Perm) (b) DC coefficient histogram of test Image (Perm).

(a)

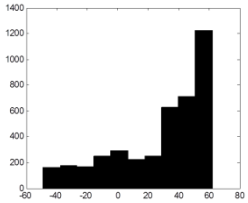

(b)

FIGURE 4: (a) Test Image (Arts) (b) DC coefficient histogram of test Image (Arts).

33	34	37	37	33	29	32	38
35	32	32	33	33	32	33	37
39	33	29	31	33	33	33	35
42	36	33	33	33	32	33	36
37	37	37	38	35	32	36	43
31	34	39	41	39	36	40	47
31	33	38	43	43	39	38	41
36	35	38	43	45	39	33	31

(a) The dark 8×8 block of test image in spatial domain

-46	0	0	0	0	0	0	0
-1	0	1	0	0	0	0	0
0	0	-1	0	0	0	0	0
0	0	0	-1	0	0	0	0
0	0	0	0	0	0	0	0
0	0	0	0	0	0	0	0
0	0	0	0	0	0	0	0
0	0	0	0	0	0	0	0

(b) The dark 8×8 block of test image in frequency domain

FIGURE 5: Dark 8×8 block of a test image.

234	237	233	229	229	228	228	225
235	232	228	229	229	226	224	226
231	231	228	229	222	215	209	199
230	226	213	198	193	178	172	176
218	199	184	174	174	168	166	173
189	163	162	166	169	179	182	180
172	167	170	176	177	176	178	188
171	169	182	195	185	191	186	186

(a) The bright 8×8 block of test image in spatial domain

36	3	1	0	0	0	0	0
14	3	0	0	0	0	0	0
3	-4	-1	0	0	0	0	0
-3	-1	1	0	0	0	0	0
0	1	0	0	0	0	0	0
0	0	0	0	0	0	0	0
0	0	0	0	0	0	0	0
0	0	0	0	0	0	0	0

(b) The bright 8×8 block of test image in frequency domain

FIGURE 6: Bright 8×8 block of a test image.

2.1 Enhancement Procedure

Let $EI = \{EI_1, EI_2, \ldots, EI_l\}$ be the set of l number of 8×8 blocks of embedded image. Let $EM = \{((1,1),(1,2),(2,1)),((1,8),(1,7),(2,8)),((8,1),(8,2),(7,1)),((8,8),(8,7),(7,8))\}$ be set of four corner coordinates of block EI_i. We considered the corner coordinates set EM, since using S. Gujjunoori et al. schemes [6, 7] we observed that there exists more repetitive distortions in smoother dark and bright regions. We enhance pixels at these coordinates of all the blocks EI_i of smoother regions based on the threshold values T_d and T_b for dark and bright regions in following two equations (2) and (3) respectively. The following reversible enhancement functions are designed by considering the distortions by S. Gujjunoori et al. schemes [6, 7] in the gray scale image.

$$EnhDark\big(EI_i(p,q),\ EI_i(m,n)\big) = \begin{cases} EI_i(m,n) = EI_i(p,q) mod 2,\ EI_i(p,q) = \lfloor EI_i(p,q)/2 \rfloor & if\ (EI_i(m,n) = 0), \\ EI_i(m,n) = EI_i(m,n) + 1 & otherwise \end{cases} \quad (2)$$

where,

$\big((p,q),(m,n),(u,v)\big) \in EM$

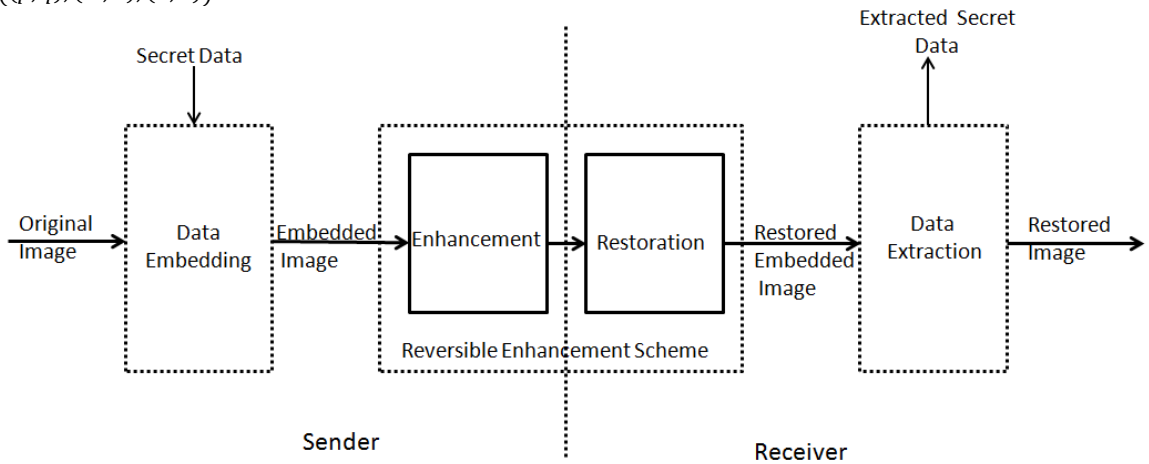

FIGURE 6: The position of reversible enhancement scheme during data embedding and extraction.

$$EnhBright\big(EI_i(p,q),\ EI_i(m,n),\ EI_i(u,v)\big) = \begin{cases} EI_i(m,n) = EI_i(m,n) + 15,\ EI_i(u,v) = EI_i(u,v) + 15,\ EI_i(p,q) = EI_i(p,q) + 1 & if\ (cond1) and\ (cond2), \\ EI_i(p,q) = EI_i(p,q) + 1 & if\ \ (EI_i(p,q) = 254), \\ \perp & otherwise \end{cases} \quad (3)$$

where,

$cond1 = (\ EI_i(p,q) = 255),\ cond2 = (\ EI_i(m,n) \leq 236) || \ EI_i(u,v) \leq 236) and \perp indicates\ \ no\ action.$

The enhancement algorithm is present in Algorithm 1.

Algorithm 1: Algorithm of Enhancement

Input : $EI = \{EI_1, EI_2, \cdots, EI_l\}$ be the set embedded image blocks.

Output: $EN = \{EN_1, EN_2, \cdots, EN_l\}$ be the set enhanced image blocks.

```
foreach EI_i ∈ EI do
    if D_i ≤ T_d then
        Enhance the dark block using (2) and store in EN_i ;
    else
        if D_i ≥ T_b then
            Enhance the bright block using (3) and store in EN_i;
        else
            EN_i = EI_i ;
            continue ;
        end
    end
end
Combine all the EN_i blocks into EN̂ ← {EN_1, EN_2, ··· , EN_l};
```

2.2 Restoration Procedure

Restoration procedure is the reverse of enhancement procedure. In this procedure, the pixels which are modified to reduce the white noise and dark spots are restored back, by using the functions in equation (4) and (5). Let $\hat{R} = \{R_1, R_2, \dots, R_l\}$ be the set of restored embedded blocks. We use the functions $RestDark$ and $RestBright$ for restoration of dark and bright regions of EN respectively, as in equations (4) and (5).

$$RestDark\big(EI_i(p,q),\ EI_i(m,n)\big) = \begin{cases} EI_i(p,q) \times 2 + EI_i(m,n),\ EI_i(m,n) = 0 & if\ (cond3)||\ (cond4) \\ EI_i(m,n) = EI_i(m,n) - 1 & otherwise \end{cases} \quad (4)$$

where,

$cond3 = (EI_i(m,n) = 0),\ EI_i(m,n) = 1)$

$$RestBright\big(EI_i(p,q),\ EI_i(m,n),\ EI_i(u,v)\big) = \begin{cases} EI_i(m,n) = EI_i(m,n) - 15,\ EI_i(u,v) = EI_i(u,v) - 15,\ EI_i(p,q) = EI_i(p,q) + 1 & if\ (EI_i(p,q) = 254), \\ EI_i(p,q) = EI_i(p,q) - 1 & if\ (EI_i(p,q) = 255), \\ \perp & otherwise \end{cases} \quad (5)$$

The algorithm for restoration is present in Algorithm 2.

Algorithm 2: Algorithm of Restoration

Input : $EN = \{EN_1, EN_2, \cdots, EN_l\}$ be the set embedded image blocks.

Output: $R = \{R_1, R_2, \cdots, R_l\}$ be the set enhanced image blocks.

```
foreach EN_i ∈ EN do
    if D_i ≤ T_d then
        Restore the dark enhanced block using (4) and store in R_i ;
    else
        if D_i ≥ T_b then
            Restore the bright enhanced block using (5) and store in R_i ;
        else
            R_i = EN_i ;
            continue ;
        end
    end
end
Combine all the R_i blocks into R̂ ← {R_1, R_2, ··· , R_l};
```

3. RESULTS AND DISCUSSION

We compare proposed enhancement scheme with S. Gujjunoori et al. schemes [6, 7] for showing how the visual quality is improved. We used 512×512 JPEG images in the implementation. From the experiment, we observed that DC threshold values T_d and T_b in Table 1 provides better choice for choosing dark and bright blocks for enhancement. We measure the visual quality in terms of metrics PSNR, PSNR-HVS, PSNR-HVS-M and SSIM-INDEX. From the Figures 11 - 14, we can observe that the visual quality is improved in terms of PSNR, SSIM-INDEX, PSNR-HVS and PSNR-HVS-M. Note that scheme1 and scheme2 in Figures 11 - 14 and Table 2 denotes S. Gujjunoori et al. scheme [6] and S. Gujjunoori et al. scheme [7] respectively. The detailed results can be found in Table 2. Note that the embedding capacity in both the schemes [6, 7] is same.

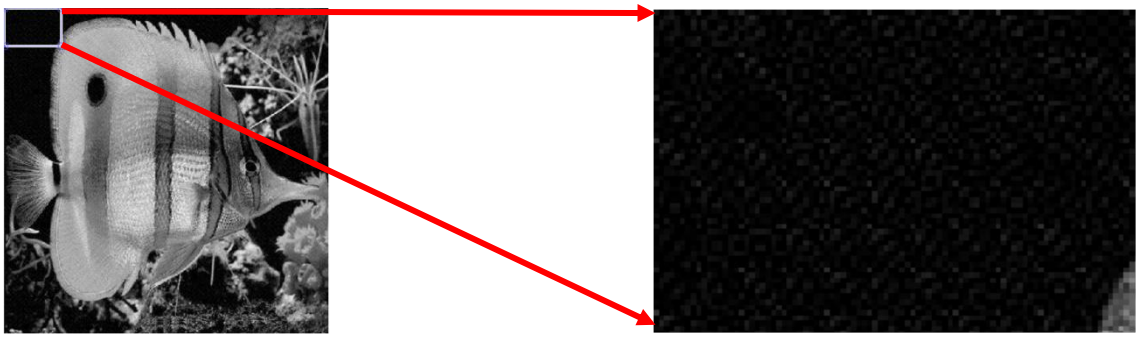

(a) (b)

FIGURE 8: (a) Fish watermarked image of S. Gujjunoori et al. scheme [7] (b) A dark block.

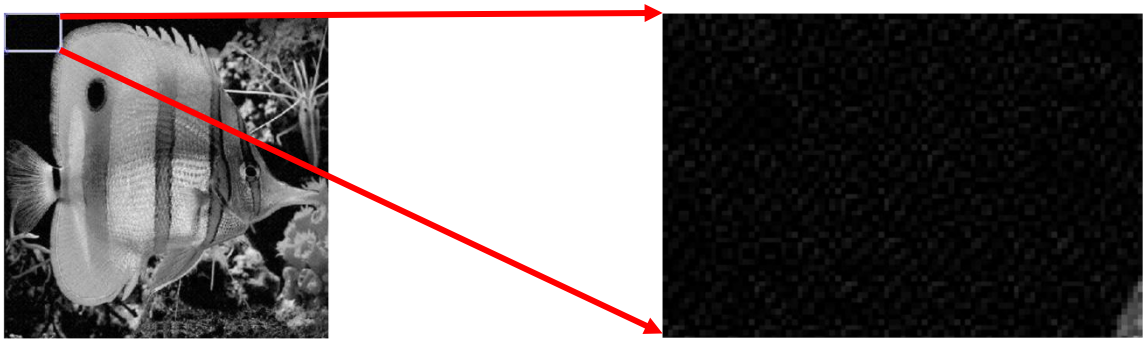

(a) (b)

FIGURE 9: (a) Enhanced fish image of proposed scheme (b) A dark enhanced block.

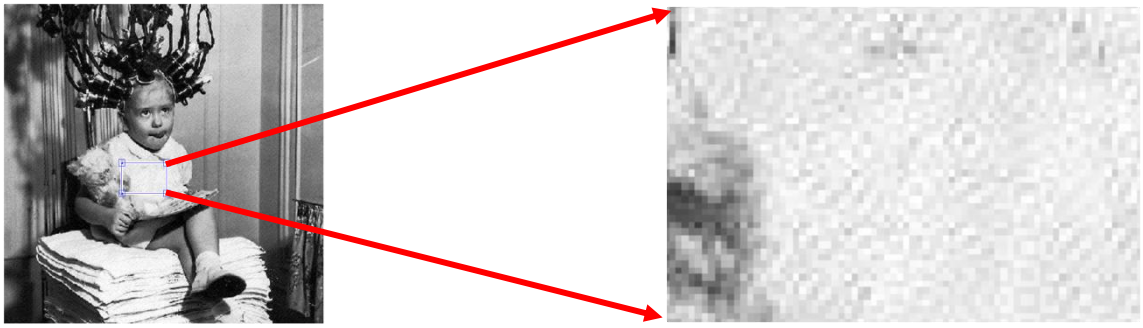

(a) (b)

FIGURE 10: (a) Perm watermarked image of S. Gujjunoori et al. scheme [7] (b) A bright block.

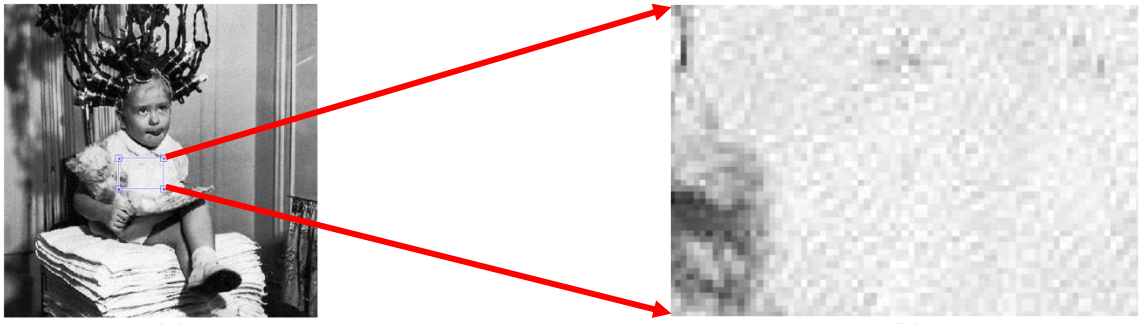

(a) (b)

FIGURE 11: (a) Enhanced perm image of proposed scheme (b) A bright block.

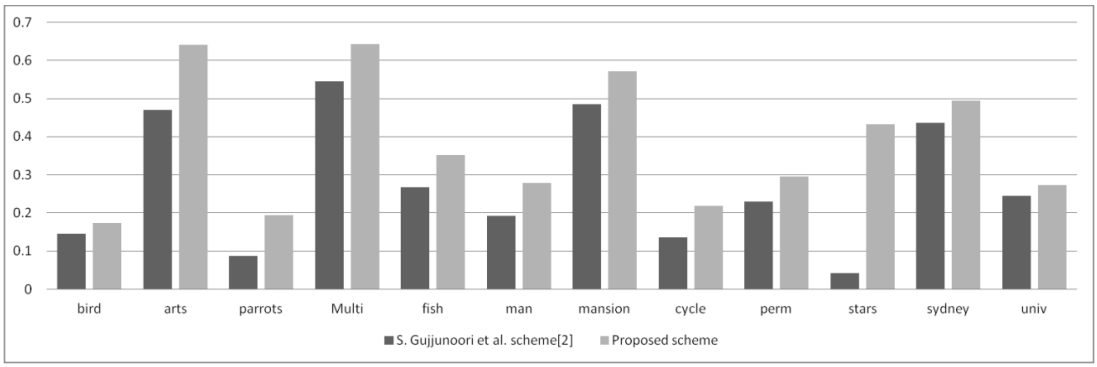

FIGURE 12: Visual quality in terms of PSNR.

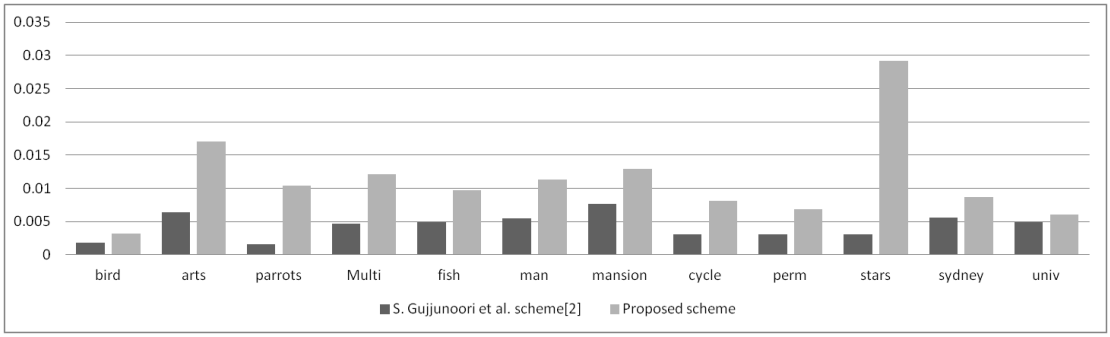

FIGURE 13: Visual quality in terms of SSIM.

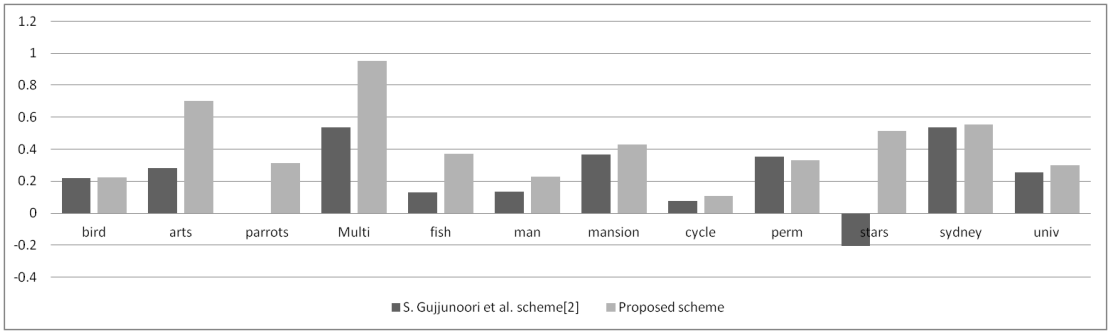

FIGURE 14: Visual quality in terms of PSNR-HVS.

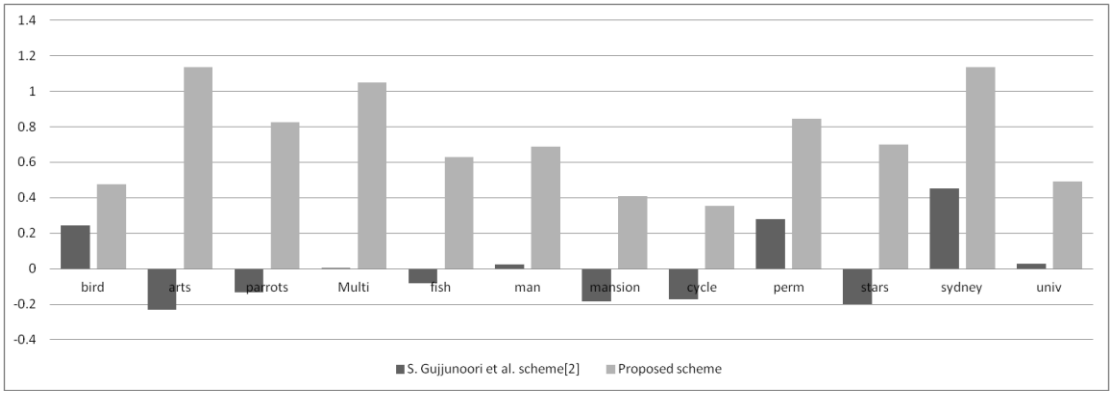

FIGURE 15: Visual quality in terms of PSNR-HVS-M.

TABLE 2: Visual quality measured in terms of PSNR, PSNR-HVS, PSNR-HVS-M, and MSSIM maintaining the CAPACITY.

Test images	Metrics	S. Gujjunoori et al. scheme [6]	S. Gujjunoori et al. scheme [7]	Proposed scheme
Bird	PSNR	26.3131	26.4591	26.487
	SSIM-INDEX	0.6413	0.6431	0.6445
	PSNR-HVS-M	43.8525	44.0971	44.3284
	PSNR-HVS	34.1097	34.3298	34.3353
Arts	PSNR	26.9131	27.3838	27.5546
	SSIM-INDEX	0.7209	0.7273	0.7379
	PSNR-HVS-M	43.8525	44.0971	44.3284
	PSNR-HVS	34.1097	34.3298	34.3353
Parrots	PSNR	26.6671	26.755	26.862
	SSIM-INDEX	0.4997	0.5013	0.5101
	PSNR-HVS-M	38.0007	37.8669	38.8268
	PSNR-HVS	33.091	33.0898	33.4043
Multi	PSNR	26.857	27.4016	27.5
	SSIM-INDEX	0.683	0.6877	0.6951
	PSNR-HVS-M	37.2074	37.2119	38.2574
	PSNR-HVS	32.42	32.955	33.3712
Fish	PSNR	26.741	27.0076	27.0921
	SSIM-INDEX	0.6893	0.6942	0.699
	PSNR-HVS-M	37.0269	36.9429	37.6545
	PSNR-HVS	32.5713	34.3711	34.2005
Man	PSNR	26.6731	26.8658	26.951
	SSIM-INDEX	0.6406	0.6461	0.6519
	PSNR-HVS-M	39.4094	39.4328	40.0963
	PSNR-HVS	33.1688	33.3042	33.3969
Mansion	PSNR	26.3821	26.8663	26.9529
	SSIM-INDEXX	0.7564	0.7641	0.7693
	PSNR-HVS-M	39.9685	39.7862	40.3767
	PSNR-HVS	33.0567	33.4869	33.6107
Cycle	PSNR	26.5727	26.7094	26.7913
	SSIM-INDEX	0.6714	0.6745	0.6795
	PSNR-HVS-M	41.6176	41.4438	41.9705
	PSNR-HVS	33.6107	33.6877	33.7178
Perm	PSNR	26.4995	26.7298	26.7958
	SSIM-INDEX	0.6785	0.6816	0.6853
	PSNR-HVS-M	43.715	43.9961	44.5582
	PSNR-HVS	33.5887	33.9404	33.9188
Stars	PSNR	28.5055	28.548	28.9375
	SSIM-INDEX	0.4716	0.4747	0.5008
	PSNR-HVS-M	31.9825	31.784	32.6824
	PSNR-HVS	30.5739	30.3705	31.0897
Sydney	PSNR	26.2924	26.7289	26.7865
	SSIM-INDEX	0.7175	0.7231	0.7262
	PSNR-HVS-M	41.5654	42.0193	42.702
	PSNR-HVS	33.248	33.7851	33.8037
Univ	PSNR	26.3302	26.5742	26.6031
	SSIM-INDEX	0.6655	0.6699	0.6711
	PSNR-HVS-M	43.8064	43.8347	44.2978
	PSNR-HVS	33.878	34.1349	34.1754

4. CONCLUSION

There is need of reversible enhancement schemes specific to an embedding scheme that may reveal the existence of hidden data, neglecting the visual quality by focusing on only other requirements such as capacity, underlying features of image during embedding. It is desirable to have a reversible enhancement scheme for sensitive applications like satellite, medical, etc. for visual inspection. To best of our knowledge this is the first work which is useful for improving the capacity by maintaining a good visual quality.

5. REFERENCES

[1] W. Bender, D. Gruhl, N. Morimoto, and A. Lu., "Techniques for data hiding" IBM Systems Journal, vol. 35(3.4), 313-336, 1996.

[2] Chi-Kwong Chan and L.M. Cheng, "Hiding data in images by simple LSB substitution," Pattern Recognition, vol. 37(3), pp. 469-474, March 2004.

[3] Dinu Coltuc and Jean-Marc Chassery, "Very fast watermarking by reversible contrast mapping," IEEE Signal Processing Letters, vol. 14(4), 255-258, April 2007.

[4] Ingemar Cox, Matthew Miller, Jeffery Bloom, J. Fridrich, and T. Kalker, "Digital watermarking and steganography," Morgan Kaufman, November 2007.

[5] Ming Sun Fu and Oscar C Au, "Data hiding watermarking for halftone images," IEEE Transactions on Image Processing, vol. 11(4), pp. 477-484, April 2002.

[6] S. Gujjunoori and B. Amberker, "DCT based reversible data embedding for mpeg-4 video using HVS Characteristics," Information Security and Applications, vol. 18(4), pp. 157-166, December 2013.

[7] S. Gujjunoori and B. Amberker., "A reversible data embedding scheme for mpeg-4 video using HVS Characteristics," Intelligent System and Signal Processing (ISSP), pp.117 -121, March 2013.

[8] Chiou-Ting Hsu and Ja-Ling Wu., "DCT-based watermarking for video," IEEE Transactions on Consumer Electronics, vol. 44(1), pp. 206-216, 1998.

[9] Xiaolong Li, Bin Yang, and Tieyong Zeng, "Efficient reversible watermarking based on adaptive prediction-error expansion and pixel selection," IEEE Transactions on Image Processing, vol. 20(12), pp. 3524-3533, January 2011.

[10] S. D. Lin and Chin-Feng Chen, "A robust DCT-based watermarking for copyright protection," IEEE Transactions on Consumer Electronics, vol. 46(3), pp. 415-421, 2000.

[11] Zhicheng Ni, Yun-Qing Shi, Nirwan Ansari, and Wei Su, "Reversible data hiding," IEEE Tran sactions on Circuits and Systems for Video Technology, vol. 16(3), pp. 354-362, March 2006.

[12] Vasiliy Sachnev, Hyoung Joong Kim, Jeho Nam, Sundaram Suresh, and Yun Qing Shi Shi., "Reversible watermarking algorithm using sorting and prediction," IEEE Transactions on Circuits Systems for Video Technology, vol. 19(7), pp. 989-999, July 2009.

[13] David Salomon, "Data compression: the complete reference," Springer Verlag, 2007.

[14] M. D. Swanson, B. Zhu, and A. H. Tewfik., "Robust data hiding for images," pp. 37-40, 1996.

[15] Diljith M. Thodi and Jeffery J. Rodriguez, "Expansion embedding techniques for reversible watermarking," IEEE Transactions on Image Processing, vol. 16(3), pp. 721-730, March 2007.

[16] Jun Tian, "Reversible data embedding using a difference expansion," IEEE Transactions on Circuits and Systems for Video Technology, vol. 13(8), pp. 890-896, August 2003.

[17] Hao-Tian Wu and Jiwu Huang, "Reversible image watermarking on prediction error by efficient histogram modification," Signal Processing, vol. 92(12), pp. 3000-3009, December 2012.

[18] Hao-Tian Wu, Jean-Luc Dugelay, and Yun-Qing Shi, “Reversible image data hiding with contrast enhancement,” IEEE Signal Processing Letters, vol. 22(1), pp. 81- 85, January 2015.

[19] Zhenfei Zhao, Hao Luo, Zhe-Ming Lu, and Jeng-Shyang Pan, “Reversible data hiding based on multilevel histogram modification and sequential recovery,” International Journal of Electronics and Commununications (AEU), vol. 65, pp. 814-826, 2011.